Multistatic target classification with adaptive waveforms

Thomas B. Butler, *Student Member, IEEE,* Nathan A. Goodman, *Senior Member, IEEE*

Department of Electrical and Computer Engineering, The University of Arizona
1230 E. Speedway Blvd., Tucson, AZ 85721
phone: + (1) 520-621-4462, fax: + (1) 520-621-8076, email: butlert@email.arizona.edu

***Abstract*—Traditional radar systems rely on a predefined suite of waveforms and post-measurement signal processing to achieve such goals as target detection, classification, and tracking. Cognitive radar (CR) is a newly proposed framework in which the radar actively interrogates the propagation channel and adapts its operating parameters in order to maximize performance. We apply CR to a target classification problem by calculating custom waveforms that maximize the information received from the target echoes. A new MIMO waveform is proposed which maximizes the mutual information between a Gaussian random target and the received data under AWGN. The results indicate that the new frequency-domain formulation offers superior performance compared to both a non-adaptive approach and an *ad hoc* application of spectral waterfilling to the MIMO setting.**

I. Introduction

Bell applied information-theoretic principles in [1] to prove that the maximum mutual information between a Gaussian-distributed target impulse response and the received target echoes, given the transmitted waveform, was achieved via a spectral waterfilling approach. Since Bell's work was published, waveform design criteria based on optimizing SINR have also emerged. Pillai, et al. [2] found an eigenfunction yielding the optimum-SINR waveform for target detection. This solution has been extended to an N-target identification problem [3] and to include colored noise and non-zero colored clutter [4].

Bell's information-theoretic approach has also received extensive treatment. Leshem, Naparstek, and Nehorai [5] developed a waterfilling technique for resolving and tracking multiple targets using multiple antenna beams, each with a different temporal waveform. Yang and Blum [6] developed an optimum time-domain solution for MIMO radars which maximizes the mutual information between a multistatic Gaussian target impulse response and the MIMO received signal vector. Unfortunately, it is not clear how to use the results of [6] to obtain the Toeplitz matrix structure necessary for a physical waveform.

The concept of intelligent surveillance systems has grown in parallel to the development of adaptive waveforms. Traditional radar systems rely on a predefined suite of waveforms and post-measurement signal processing to achieve such goals as target detection, classification, and tracking. These systems must therefore adapt to difficult or complex propagation environments in a reactive, *post hoc* manner. Cognitive radar (CR) is a newly proposed concept [7] wherein the radar proactively interrogates the radar channel and adapts its parameters in real-time. CR depends upon a Bayesian model of the radar channel [7], [8] to iteratively update its knowledge—and act upon that knowledge—with each transmission. For example, a CR system can accomplish target recognition very efficiently by adapting its transmitted waveforms to maximize mutual information based on all prior knowledge. In such a scheme, the system develops custom radar waveforms based on previously received information and iteratively updates target classification likelihoods until a hard decision can be made. It has been shown that such a sequential hypothesis testing (SHT) approach results in correct target recognition in a monostatic setting with fewer waveform transmissions—and therefore less expended time and energy—than for a non-adaptive approach [9].

In this paper, we extend the adaptive-waveform SHT approach to include bistatic target echoes in a multiple-input, multiple-output (MIMO) radar system. We introduce a frequency-domain MIMO waveform that optimizes mutual information, between a Gaussian target process and the received data. This approach is applied sub-optimally to the target identification problem under both deterministic and random target models, and the results are compared to *ad hoc* extensions of the waterfilling solution presented in [9].

II. Frequency-domain waveform design for Single-Input, Multiple-Output (SIMO) systems

A. Signal Model

The derivations in this section assume a single-input, multiple-output (SIMO) system consisting of one co-located transmitter/receiver pair and a set of receivers located elsewhere. In Section III, a MIMO formulation is explored.

Let the $K \times 1$ vector $\mathbf{X}$ represent the spectrum of a transmitted waveform vector at K discrete frequencies across the waveform's bandwidth. Likewise, $\mathbf{G}_q$ shall represent the target transfer function for the path between the transmitter and qth receiver, and the received waveform at receiver q shall be denoted by $\mathbf{Y}_q$. For notational convenience, we also define $\chi = \mathrm{diag}(\mathbf{X})$ such that the spectral components of

1-4244-1539-X/08/$25.00 ©2008 IEEE

the waveform reside on the diagonal of χ (the diag operation places an N-element vector on the diagonal of an $N \times N$ matrix, with zeros in all other positions of the matrix).

From the forgoing, we can see that the received vector $\mathbf{Y}$ under AWGN can be expressed as

$$\mathbf{Y} = \begin{bmatrix} \mathbf{Y}_1 \\ \mathbf{Y}_2 \\ \vdots \\ \mathbf{Y}_Q \end{bmatrix} = \begin{bmatrix} \chi\mathbf{G}_1 + \mathbf{N}_1 \\ \chi\mathbf{G}_2 + \mathbf{N}_2 \\ \vdots \\ \chi\mathbf{G}_Q + \mathbf{N}_Q \end{bmatrix}. \tag{1}$$

The noise vectors $\mathbf{N}_q$ are assumed to be zero-mean complex Gaussian-distributed random vectors with covariance matrix $\mathbf{I}$. The transfer functions $\mathbf{G}_q$ may be random or deterministic, depending on the problem being considered.

B. Optimum waveform for Gaussian random target

In this formulation, we assume that the target transfer function $\mathbf{G}_q$ in (1) is a zero-mean complex Gaussian process with covariance matrix $\mathbf{K}_q = \mathrm{E}\left[\mathbf{G}_q\mathbf{G}_q^{\mathrm{H}}\right] = \mathrm{diag}(\Psi_q(f_k))$, where $\Psi_q(f_k)$ is the power spectral density for the path between the transmitter and receiver q. We define the total system transfer function $\mathbf{G} = [\mathbf{G}_1^{\mathrm{T}}, \ldots, \mathbf{G}_Q^{\mathrm{T}}]^{\mathrm{T}}$ with covariance matrix $\mathbf{K} = \mathrm{blkdiag}\,(\mathbf{K}_1, \ldots, \mathbf{K}_Q)$, where the $\mathrm{blkdiag}$ operator creates a block-diagonal matrix of its matrix arguments. Our goal is to calculate a waveform $\mathbf{X}$ that maximizes the mutual information between the bistatic target transfer function, $\mathbf{G}$, and the received signal vector $\mathbf{Y}$. Therefore, we have

$$I\left(\mathbf{G}; \mathbf{Y}\right) = H\left(\mathbf{Y}\right) - H\left(\mathbf{Y}|\mathbf{G}\right). \tag{2}$$

where $H()$ refers to the entropy of a random vector.

First, we will evaluate $H\left(\mathbf{Y}|\mathbf{G}\right)$. Given the bistatic target transfer function, the only random component of the received signal vector is the AWGN. Therefore, the received data in this case are Gaussian with a mean of $\mathbf{XG}$ and variance of σ^2. The entropy of such a random vector is

$$H\left(\mathbf{Y}|\mathbf{G}\right) = \log\left\{\left(\pi e\right)^{QK}\left|\sigma^2\mathbf{I}_{QK}\right|\right\}. \tag{3}$$

When not conditioned on a target transfer function, $\mathbf{Y}$ is zero-mean Gaussian with covariance $\mathbf{R} = \chi\mathbf{K}\chi^{\mathrm{H}} + \sigma^2\mathbf{I}_{QK}$, and so the entropy is

$$H\left(\mathbf{Y}\right) = \log\left\{\left(\pi e\right)^{QK}\left|\mathbf{R}\right|\right\}. \tag{4}$$

Substituting (3) and (4) into (2), we obtain

$$I\left(\mathbf{G}; \mathbf{Y}\right) = \sum_{k=1}^{K}\sum_{q=1}^{Q}\log\left\{1 + \frac{\left|X\left(f_k\right)\right|^2\Psi_q\left(f_k\right)}{\sigma^2}\right\}. \tag{5}$$

Next, we maximize (5) by the Lagrange technique with the constraint on total transmitted energy according to

$$\sum_{k=1}^{K}\left|X\left(f_k\right)\right|^2 = E_s. \tag{6}$$

Letting $P_k = \left|X\left(f_k\right)\right|^2$, we can write the objective function as

$$J = \sum_{k=1}^{K}\sum_{q=1}^{Q}\log\left\{1 + \frac{P_k\Psi_q\left(f_k\right)}{\sigma^2}\right\} + \lambda\sum_{k=1}^{K}P_k. \tag{7}$$

The derivative of (7) with respect to P_k is

$$\begin{aligned}\frac{\partial J}{\partial P_k} &= \sum_{q=1}^{Q}\frac{\Psi_q\left(f_k\right)/\sigma^2}{1 + P_k\Psi_q\left(f_k\right)/\sigma^2} + \lambda \\ &= \sum_{q=1}^{Q}\frac{\Psi_q\left(f_k\right)}{\sigma^2 + P_k\Psi_q\left(f_k\right)} + \lambda.\end{aligned} \tag{8}$$

We solve for P_k by equating (8) to zero and assuming an arbitrary value for λ. A set of powers P_k that satisfy (6) is then found by a numerical search for the correct λ. In the case of a single receiver ($Q = 1$), this solution reduces to the waterfilling solution presented in [1] and [9]. However, for $Q > 1$, the solution does not reduce to a waterfilling form.

1) Application to the multi-hypothesis case with deterministic targets: The foregoing derivation yields an optimum frequency-domain waveform under AWGN and a zero-mean Gaussian random target model, but we require the ability to calculate custom waveforms for a finite set of known target hypotheses and deterministic transfer functions $\mathbf{G}_q(H_m)$. To this end, we apply the optimization technique in a sub-optimal manner by interpreting the set of power spectral densities $\Psi_q(f)$ in (8) as a spectral variance over the target set. For each path q through the SIMO system, we calculate the spectral variance to be

$$\begin{aligned}\sigma_{g:q}^2(f_k) &= \Psi_q(f_k) \\ &= \sum_{m=1}^{M}\left|G_{q,m}(f_k)\right|^2 P_m - \left|\sum_{m=1}^{M}G_{q,m}(f_k)P_m\right|^2\end{aligned} \tag{9}$$

where $G_{q,m}(f_k)$ is the transfer function at frequency f_k under hypothesis H_m for path q.

2) Application to the multi-hypothesis case with random targets: We must modify the spectral variance given in (9) if we wish to model random targets with zero-mean Gaussian transfer functions $\tilde{\mathbf{G}}_q(H_m)$. In this case, each hypothesis is a class of targets with realizations that depend on the class statistics. Hence, we do not have known transfer functions, but instead model each class as having a PSD for each bistatic path. The form of (9) suggests a random-model counterpart given by

$$\begin{aligned}\sigma_{g:q}^2(f_k) &= \Psi_q(f_k) \\ &= \sum_{m=1}^{M}\Psi_{q,m}(f_k)P_m - \left(\sum_{m=1}^{M}\sqrt{\Psi_{q,m}(f_k)}P_m\right)^2\end{aligned} \tag{10}$$

where $\Psi_{q,m}(f_k)$ is the power spectral density at the kth frequency for the mth hypothesis over the qth path. In this way, we can model the target transfer functions $\tilde{\mathbf{G}}_q(H_m)$

under hypothesis H_m each as zero-mean complex Gaussian-distributed random vectors with covariance matrix $\mathbf{K}_q(H_m) = \mathrm{diag}(\Psi_{q,m}(f))$. For later notational convenience, we define a covariance matrix $\mathbf{K}(H_m)$ which accounts for all receivers under hypothesis H_m, taking the form

$$\mathbf{K}(H_m) = \mathrm{blkdiag}\left(\mathbf{K}_1(H_m), \ldots, \mathbf{K}_Q(H_m)\right). \tag{11}$$

C. Bistatic waterfilling waveform

We develop an *ad hoc* bistatic, frequency-domain waterfilling solution similar to the solution presented in [9]. In this method, we sum the spectral variance over all paths as

$$\sigma_g^2(f_k) = \sum_{q=1}^{Q} \sigma_{g:q}^2(f_k) \tag{12}$$

where $\sigma_{g:q}^2(f_k)$ is the spectral variance for the qth SIMO path given in (9) or (10). The waterfilling solution for the transmit spectrum $\mathbf{X}$ is given by

$$|X(f_k)|^2 = \left(A - \frac{\sigma^2 K}{2\sigma_g^2(f_k)}\right)^+ \tag{13}$$

subject to the same energy constraint given in (6). The '+' operator is defined such that $(a)^+ = \max[0, a]$.

III. Frequency-domain waveform design for Multiple-Input, Multiple-Output (MIMO) systems

A. Signal Model

A frequency-domain MIMO signal model similar to the SIMO case discussed in Section II is developed here. We begin by denoting the target transfer function between transmitter p and receiver q as

$$\mathbf{G}_{p,q} = [G_{p,q}(f_1), \ldots, G_{p,q}(f_K)]^{\mathrm{T}}. \tag{14}$$

All transfer functions for transmitter p can be grouped into a vector taking the form

$$\mathbf{G}_p = [\mathbf{G}_{p,1}^{\mathrm{T}}, \ldots, \mathbf{G}_{p,Q}^{\mathrm{T}}]^{\mathrm{T}}, \tag{15}$$

and the transfer functions for all transmitters are collected into a $PQK \times 1$ vector

$$\mathbf{G} = [\mathbf{G}_1^{\mathrm{T}}, \ldots, \mathbf{G}_P^{\mathrm{T}}]^{\mathrm{T}}. \tag{16}$$

Because the transfer functions are grouped by transmitter, the transmitted waveform spectrum takes the form

$$\begin{aligned}\mathbf{X} = \ & [\ \mathbf{X}_1^{\mathrm{T}}\ \ \mathbf{X}_1^{\mathrm{T}}\ \ \ldots\ \ \mathbf{X}_1^{\mathrm{T}} \\ & \ldots\ \ \mathbf{X}_P^{\mathrm{T}}\ \ \ldots\ \ \mathbf{X}_P^{\mathrm{T}}\ ]^{\ \mathrm{T}},\end{aligned} \tag{17}$$

where the vectors $\mathbf{X}_p$ represent the waveform transmitted by transmitter p. In (17), each $\mathbf{X}_p$ is repeated Q times in order to form the vector $\mathbf{X}$.

The received $PQK \times 1$ data vector is then denoted as

$$\mathbf{Y} = \chi\mathbf{G} + \mathbf{N}. \tag{18}$$

where $\chi = \mathrm{diag}(\mathbf{X})$ and $\mathbf{N}$ is AWGN with covariance matrix $\sigma^2\mathbf{I}_{PQK}$.

B. Optimum waveform for Gaussian random target

Here we develop a MIMO extension of the SIMO waveform discussed in Section II-B. Much of the derivation is identical, except the vectors and matrices take the MIMO form given in Section III-A. The zero-mean Gaussian transfer function between transmitter p and receiver q is denoted by $\mathbf{G}_{p,q}$, which takes the form of (14) and has covariance matrix $\mathbf{K}_{p,q} = \mathrm{diag}(\Psi_{p,q}(f))$. The system transfer function $\mathbf{G}$ is therefore given by (16) and has covariance matrix $\mathbf{K} = \mathrm{blkdiag}(\mathbf{K}_{p,q})$.

Following the same logic as the SIMO derivation, and letting $P_{p,k} = |X_p(f_k)|^2$, we must solve

$$\frac{\partial J}{\partial P_{p,k}} = \sum_{q=1}^{Q} \frac{\Psi_{p,q}(f_k)}{\sigma^2 + P_{p,k}\Psi_{p,q}(f_k)} + \lambda = 0, \quad 1 \le p \le P \tag{19}$$

subject to the constraint

$$\sum_{p=1}^{P}\sum_{k=1}^{K} |X_p(f_k)|^2 = E_s. \tag{20}$$

The procedure for solving (19) is similar to the procedure for solving (8).

1) Application to the multi-hypothesis case with deterministic targets: The deterministic target spectral variance can be extended to a MIMO system by slightly modifying of the notation in (9) to include an index for transmitter p. We can write

$$\begin{aligned}\sigma_{g:p,q}^2(f_k) &= \Psi_{p,q}(f_k) \\ &= \sum_{m=1}^{M} |G_{p,q,m}(f_k)|^2 P_m - \left|\sum_{m=1}^{M} G_{p,q,m}(f_k)P_m\right|^2,\end{aligned} \tag{21}$$

where $G_{p,q,m}(f)$ is the transfer function over the path from transmitter p to receiver q under hypothesis H_m.

2) Application to the multi-hypothesis case with random targets: To apply this signal model to a set of random targets, we need to interpret each transfer function $\mathbf{G}_{p,q}$ defined in (14) as a zero-mean Gaussian-distributed random vector $\tilde{\mathbf{G}}_{p,q}(H_m)$ under hypothesis H_m. The random transfer function has covariance matrix $\mathbf{K}_{p,q}(H_m) = \mathrm{diag}(\Psi_{p,q,m}(f_k))$, where $\Psi_{p,q,m}(f_k)$ is the target power spectral density under hypothesis H_m for the pth transmitter and the qth receiver. The grouped transfer function $\tilde{\mathbf{G}}_p(H_m)$ with structure similar to (15) therefore has a $PQK \times PQK$ covariance matrix

$$\mathbf{K}(H_m) = \mathrm{blkdiag}(\mathbf{K}_{p,q}(H_m)). \tag{22}$$

We then calculate the spectral variance to be

$$\begin{aligned}&\sigma_{g:p,q}^2(f_k) = \Psi_{p,q}(f_k) \\ &= \sum_{m=1}^{M} \Psi_{p,q,m}(f_k)P_m - \left(\sum_{m=1}^{M} \sqrt{\Psi_{p,q,m}(f_k)}P_m\right)^2.\end{aligned} \tag{23}$$

C. MIMO waterfilling waveform

The *ad hoc* bistatic waterfilling waveform described in Section II-C is easily extended to the MIMO signal model. We define a spectral variance over the target set for transmitter p as

$$\sigma_{g:p}^2(f_k) = \sum_{q=1}^{Q} \sigma_{g:p,q}^2(f_k), \tag{24}$$

where $\sigma_{g:p,q}^2(f_k)$ is the spectral variance over the target set for the path between transmitter p and receiver q defined in (21) or (23). The waterfilling waveform $\mathbf{X}_p$ for transmitter p is then calculated according to

$$|X_p(f_k)|^2 = \left(A - \frac{\sigma^2 K}{2\sigma_{g:p}^2(f_k)}\right)^+, \ 1 \le p \le P \tag{25}$$

subject to the constraint given in (20).

We also explore an alternative constraint which divides the transmitted energy equally among the transmitters. This constraint takes the form

$$\frac{E_s}{P} = \sum_{k=1}^{K} \left(A - \frac{\sigma^2 K}{2\sigma_{g:p}^2(f_k)}\right)^+, \ 1 \le p \le P. \tag{26}$$

There is an important difference in the waveforms resulting from the constraints given in (20) and (26). Equation (20) represents a global transmit energy constraint, so it is possible for each of the p transmitters to contribute unequally to the total transmitted energy. However, (26) requires each transmitter to transmit a waveform with an equal fraction of the globally constrained energy.

IV. Sequential hypothesis testing for target classification

A. Deterministic target model

In [9], the authors present an iterative method for target classification based on the sequential probability ratio test (SPRT) [10]. We apply the SPRT under the signal models and waveform design techniques discussed previously for both SIMO and MIMO systems. For each iteration of the test, the waveform is determined via (19) or (25) and constrained by (20). The alternative constraint (26) is also explored for the MIMO waterfilling waveform.

Equation (18) defines the received data, and the likelihood ratio (LR) is calculated between each pair of target hypotheses. If the LR between a single target class and all other classes is greater than some threshold, the test is terminated. Otherwise, another iteration is performed.

In the deterministic model, the data conditioned on a given hypothesis has non-zero mean and the randomness is due only to the AWGN. Hence, the data are independent and the LR for iteration k between target hypotheses H_i and H_j is

$$\lambda_{i,j}^k = \frac{p_{i1}(\mathbf{Y}_1)p_{i2}(\mathbf{Y}_2)\dots p_{ik}(\mathbf{Y}_k)}{p_{j1}(\mathbf{Y}_1)p_{j2}(\mathbf{Y}_2)\dots p_{jk}(\mathbf{Y}_k)} \frac{P_i^1}{P_j^1}. \tag{27}$$

where p_{ik} is the pdf of the *k*th observation under the *i*th hypothesis and $\mathbf{Y}_k$ is the received waveform due to χ_k, the *k*th transmission waveform. The factor P_i^1 is the initial value assigned to the probability of target hypothesis H_i, usually $\frac{1}{M}$. Under AWGN, the pdf is

$$p_{ik}(\mathbf{Y}_k) = \frac{1}{(\pi\sigma^2)^{PQK}} \exp\left[-\frac{1}{\sigma^2}\left(\mathbf{Y}_k - \chi_k \mathbf{G}_i\right)^{\mathrm{H}} \left(\mathbf{Y}_k - \chi_k \mathbf{G}_i\right)\right]. \tag{28}$$

We define $\alpha_{i,j}$ as the average rate of making an error by choosing target hypothesis H_j when H_i is true. According to [10], the threshold for terminating the SPRT is then reached when

$$\lambda_{m,j}^k > \frac{1-\alpha_{m,j}}{\alpha_{m,j}} \quad \forall \ j \neq m \tag{29}$$

is met for some *m*. If another iteration is to be performed because (29) is not met for any *m*, the probability P_i^{k+1} of H_i in iteration $k+1$ is updated to be

$$P_i^{k+1} = \beta p_{ik}(\mathbf{Y}_k) P_i^k \tag{30}$$

for hypotheses $H_1, H_2, \dots, H_M$ where β is a constant that ensures the probabilities sum to unity. These target class probabilities are then used to calculate the new waveform for iteration $k+1$.

B. Random target model

To apply the SPRT under a random-target signal model, a different likelihood ratio test than (27) is required. The target transfer function $\mathbf{G}$ in (18) is random but remains constant for the duration of a single experiment. As a result, the received waveform spectrum $\mathbf{Y}_k$ for the kth iteration, taking the form of the left-hand side of (18), is correlated with all previous received waveform spectra $\mathbf{Y}_{k-1}, \dots, \mathbf{Y}_1$. This correlation requires the likelihood ratio between target hypotheses H_i and H_j to be expressed in terms of the joint pdf of the spectra $\mathbf{Y}_k$ as

$$\lambda_{i,j}^k = \frac{p_i(\mathbf{Y}_1, \dots, \mathbf{Y}_k)}{p_j(\mathbf{Y}_1, \dots, \mathbf{Y}_k)} \frac{P_i^1}{P_j^1}. \tag{31}$$

It can be shown that the joint pdf for the kth iteration takes the form

$$\begin{aligned} p_i(\mathbf{Y}_1, \dots, \mathbf{Y}_k) = \\ \frac{\left|\mathbf{Q}^{-1}\right|}{(\pi\sigma^2)^{kL}\left|\mathbf{K}(H_i)\right|} \exp\left[-\frac{1}{\sigma^2}\sum_{j=1}^{k} \mathbf{Y}_k^{\mathrm{H}}\mathbf{Y}_k\right] \\ \times \exp\left[\frac{1}{\sigma^4}\left(\sum_{j=1}^{k}\mathbf{Y}_k^{\mathrm{H}}\chi_k\right)\mathbf{Q}^{-1}\left(\sum_{j=1}^{k}\mathbf{Y}_k\chi_k^{\mathrm{H}}\right)\right]. \end{aligned} \tag{32}$$

where L is the length of the received spectrum vector, and $\mathbf{Q}$ is defined as

$$\mathbf{Q} = \left(\mathbf{K}(H_i)\right)^{-1} + \frac{1}{\sigma^2}\sum_{j=1}^{k} \chi_k^{\mathrm{H}}\chi_k. \tag{33}$$

Because (31) represents the a ratio of joint pdfs for all data since the beginning of the experiment, the updated class probabilities are not calculated as in (30), but instead as

$$P_i^{k+1} = \beta p_i(\mathbf{Y}_1, \ldots, \mathbf{Y}_k) P_i^1. \tag{34}$$

V. Results

A. Deterministic targets

We have obtained scattering center data for three target vehicle types for our experiments. In these models, a target is represented by sets of scattering centers parameterized by the elevation and azimuth angles relative to the target's body coordinates. Let ϕ be the elevation and θ be the azimuth. These aspect angles can then be represented by a unit vector $\mathbf{u}(\theta, \phi)$ pointing from the target coordinate origin to the radar's position.

In the scattering center model, the tuple consisting of the target class, azimuth, and elevation selects a set of scattering centers, each with a complex reflectivity voltage γ_i and position vector $\mathbf{r}_i$ relative to the target coordinate origin. The slant range from the radar to scattering center i can be expressed as

$$R_i = R_0 + \mathbf{u}(\theta, \phi) \cdot \mathbf{r}_i \tag{35}$$

where R_0 is the slant range from the radar to the target coordinate origin.

If there are N_s scattering centers, the transfer function for the one-way radar channel between transmitter p and the target is given by

$$G_p(f) = \sum_{i=1}^{N_s} \gamma_i \exp\left[-j\frac{2\pi f}{c}(R_i)\right], \quad -\frac{F_B}{2} \leq f \leq \frac{F_B}{2}, \tag{36}$$

where F_B is the complex-baseband bandwidth of the radar signal.

We extend the scattering center model into a bistatic model as follows. Let the transfer function between transmitter p and the target and the transfer function between the target and receiver q be represented by $G_p(f)$ and $G_q(f)$, respectively, with the form given by (36). Then we let the transfer function for the bistatic radar channel between transmitter p and receiver q be

$$\mathbf{G}_{p,q}(f) = G_p(f) G_q(f). \tag{37}$$

Admittedly, this bistatic formulation is non-physical and goes beyond the capabilities of the scattering center model, yet it is the closest approximation to physical reality that we were able to obtain.

The targets are considered at a fixed elevation angle and 360° of azimuth angles in two-degree increments. Thus the SPRT must distinguish between three target classes, each with 180 aspect angles, for a total of 540 hypotheses. For each trial of the experiment, a target class and aspect angle is chosen randomly, and the SPRT is applied with $\alpha = 0.01$ as discussed in Section IV-A. This experiment is repeated for 1500 trials over a range of signal energies E_s in order to determine the average number of iterations required to reach the classification threshold in (29). The AWGN power is normalized to $\sigma^2 = 1$. The modeled MIMO radar system consists of three co-located transmitter/receiver pairs illuminating a single target.

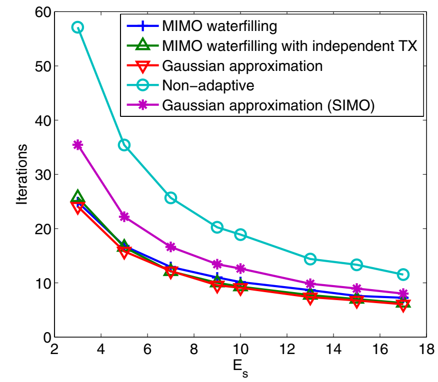

Fig. 1: Classification performance for deterministic targets

Figure 1 shows classification performance results for the deterministic target experiments. In this figure, 'MIMO waterfilling' refers to the waveform design method discussed in Section III-C using the global energy constraint given by (20). Similarly, 'MIMO waterfilling with independent TX' refers to the MIMO waterfilling waveform with the local, per-transmitter constraint given by (26). The 'Gaussian approximation' data (so named because the target set is 'approximated' as a Gaussian process) indicates the performance of a waveform designed according to Section III-B, also with the global constraint in (20). A 'Non-adaptive,' flat-spectrum waveform (time-domain impulse) is compared to the three adaptive techniques, and a SIMO case ($P = 1$, $Q = 3$) with equal energy for the Gaussian approximation waveform is provided as a final comparison.

From the figure, we can see that adaptive waveforms in a MIMO radar system provide an appreciable performance gain over both a non-adaptive impulse and over an adaptive technique employed in a SIMO system. However, no clear winner emerges from the three adaptive MIMO techniques. Figure 2 shows the error rates among the five waveforms. We find from [10] that the likelihood ratio test given by (29) only constrains the error rate α between pairs of hypotheses, and so the overall error rates can be higher than α, particularly in cases with many hypotheses. Hence the error rates shown in Figure 2 exceed α by large margins for all but the MIMO Gaussian approximation waveform. Adjusted for error rate, the MIMO Gaussian approximation waveform outperforms the other adaptive methods.

B. Random targets

In these experiments, power spectral densities (PSDs) $\Psi_{p,q}(f)$ are chosen to have spectral peaks with various shapes and varying overlap between 4 target hypotheses. For each trial of the experiment, the correct target class is chosen randomly, and its PSDs are used to color a Gaussian process to create a realization of the random transfer functions corresponding

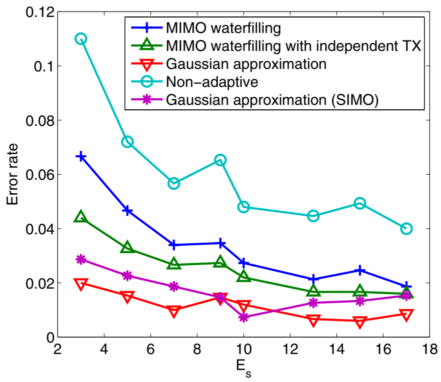

Fig. 2: Error-rate performance for deterministic targets

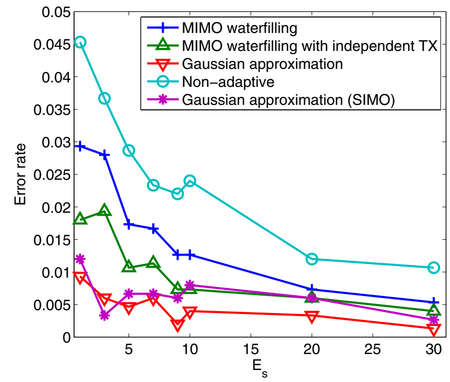

Fig. 4: Error-rate performance for random targets

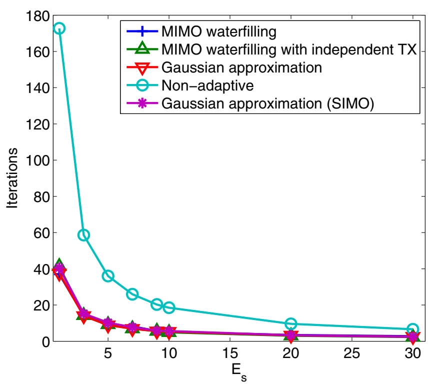

Fig. 3: Classification performance for random targets

to different paths through the MIMO system. The experiment then proceeds as in the deterministic target case, except that the SPRT described in Section IV-B governs the classification process. Figure 3 shows the results for classification performance. As was the case with the deterministic model, none of the adaptive techniques stands out as superior based on iterations for classification alone. Interestingly, the SIMO waveform does not perform much worse than its MIMO counterpart for our chosen set of PSDs. However, examination of Figure 4 reveals a similar trend as in the deterministic target case; the Gaussian approximation waveform yields the best error rate in a classification application with random targets.

VI. Conclusion

In this paper, we presented a MIMO waveform that maximizes the mutual information between a Gaussian random target and the received echo data, and this waveform was applied to a classification scenario with a finite number of target hypotheses and compared to an *ad hoc* waterfilling approach. Classification performance was investigated under two target models: a set of deterministic hypotheses from a scattering center model, and a random target model defined by a set of PSDs. While the new waveform does not classify targets in fewer iterations than either of the two waterfilling approaches, it achieves better error rates and therefore better classification accuracy. We feel that this Gaussian approximation waveform is a promising advance in the development of cognitive MIMO radar systems.

References

[1] M. R. Bell, "Information theory and radar waveform design," *IEEE Trans. Inf. Theory*, vol. 39, no. 5, pp. 1578–1597, Sep. 1993.

[2] S. Pillai, H. Oh, D. Youla, and J. Guerci, "Optimum transmit-receiver design in the presence of signal-dependent interference and channel noise," *IEEE Trans. Inf. Theory*, vol. 46, no. 2, pp. 577–584, Mar. 2000.

[3] J. R. Guerci and S. U. Pillai, "Theory and application of optimum transmit-receive radar," in *Proc. IEEE 2000 Int. Radar Conf.*, Washington, D.C., May 8–12, 2000, pp. 705–710.

[4] D. A. Garren, M. K. Osborn, A. C. Odom, J. S. Goldstein, and J. R. Guerci, "Enhanced target detection and identification via optimised radar transmission pulse shape," in *IEE Proc.–Radar, Sonar Navig.*, vol. 148, no. 3, Jun. 2001, pp. 130–138.

[5] A. Leshem, O. Naparstek, and A. Nehorai, "Information theoretic adaptive radar waveform design for multiple extended targets," *IEEE J. Sel. Topics in Sig. Proc.*, vol. 1, no. 1, pp. 42–55, Jun. 2007.

[6] Y. Yang and R. S. Blum, "Mimo radar waveform design based on mutual information and minimum mean-square error estimation," *IEEE Trans. Aerosp. Electron. Syst.*, vol. 43, no. 1, pp. 330–343, Jan. 2007.

[7] S. Haykin, "Cognitive radar: A way of the future," *IEEE Signal Process. Mag.*, vol. 23, no. 1, pp. 30–40, Jan. 2006.

[8] D. R. Fuhrmann, "Active-testing surveillance systems, or, playing twenty questions with a radar," in *Proc. 11th Annu. Adaptive Sensor and Array Processing (ASAP) Workshop*, Lexington, MA, Mar. 11–13, 2003, MIT Lincoln Lab.

[9] N. A. Goodman, P. R. Venkata, and M. A. Neifeld, "Adaptive waveform design and sequential hypothesis testing for target recognition with active sensors," *IEEE J. Sel. Topics in Sig. Proc.*, vol. 1, no. 1, pp. 105–113, Jun. 2007.

[10] P. Armitage, "Sequential analysis with more than two alternative hypotheses and its relation to discriminant function analysis," *J. R. Statist. Soc., ser. B*, vol. 12, no. 1, pp. 137–144, 1950.